ELSEVIER

Journal of Photochemistry and Photobiology A: Chemistry 134 (2000) 133–137

Journal of Photochemistry and Photobiology A:Chemistry

www.elsevier.nl/locate/jphotochem

UV absorption spectrum of BrOCl

James B. Burkholder [a,*], Gary Knight [a,1], John J. Orlando [b]

[a] *Aeronomy Laboratory, National Oceanic and Atmospheric Administration, R/AL2, 325 Broadway, Boulder, CO 80303, USA*
[b] *Atmospheric Chemistry Division, National Center for Atmospheric Research, Boulder, CO 80303, USA*

Received 4 January 2000; received in revised form 17 February 2000; accepted 29 February 2000

Abstract

The UV absorption cross sections for BrOCl in the gas phase have been measured over the wavelength range 230–390 nm. Absorption measurements were made at 298 K using a 100 cm long absorption cell and a diode array spectrometer. BrOCl was generated in the gas phase by exposing a $BrCl/Cl_2/Br_2$ gas mixture to solid HgO. The BrOCl absorption spectrum showed peaks at 272 (2.00×10^{-18} cm^2 per molecule) and 320 nm (0.574×10^{-18} cm^2 per molecule). Absorption cross sections were determined by mass balance following the decomposition of the gas mixture.

Keywords: UV absorption spectrum; BrOCl; Cross section

1. Introduction

The spectroscopy and chemistry of Cl_2O [1–4] and Br_2O [5–8] has been of interest recently due to their possible roles in atmospheric chemistry and laboratory kinetics. However, very little is known of the physical properties or reactivity for the mixed halogen species BrOCl. Lee [9] has applied ab initio methods to calculate the geometry and thermochemistry of BrOCl. Bahou et al. [10] observed BrOCl by infrared spectroscopy using the frequencies calculated by Lee following photolysis of $BrCl/O_3$ in a cold matrix. To our knowledge, BrOCl has not been identified in the gas phase.

In this work, we report the UV absorption spectrum and cross sections for BrOCl in the gas phase. Spectra were recorded using a diode array spectrometer. BrOCl was produced by applying techniques similar to those used for the laboratory production of Cl_2O and Br_2O [5,6,11].

2. Experimental

BrOCl was produced through the reaction of halogens with solid HgO. This technique has been used successfully in the past to generate gas phase samples of Cl_2O and Br_2O. BrCl (gas phase) was added to a 250 cm^3 evacuated glass flask which contained ~10 g of HgO. The flask had teflon stopcocks and was at room temperature. The BrCl sample also contained some Cl_2 and Br_2 and the total halogen pressure was in the range 5–50 Torr. It was found during our measurements that the presence of Cl_2 was required to produce BrOCl. The contact time between the gases and HgO was typically a few minutes before the gas sample was either expanded into an absorption cell or transferred to a cold trap (77 K).

The UV absorption measurements were performed using a 1024-element diode array spectrometer at both the NOAA and NCAR laboratories. The apparatus used were very similar in nature and identical results were obtained with each. The apparatus are described in detail elsewhere [12,13]. Using a diode array spectrometer enabled accurate acquisition and subsequent analysis of spectra measured over a broad wavelength range. The spectrometer bandwidths were set-up to be 165 nm (NOAA, 230–395 nm) and 250 nm (NCAR, 200–450 nm). A D_2 lamp was used for the light source and the absorption cells were nominally 3 cm i.d. with a pathlength of 100 cm.

UV absorption measurements were made in both static and flow modes. In either case absorption measurements were made by first recording the D_2 lamp spectrum, I_0, with the cell evacuated or flushed. Detector exposure times were ~0.2 s and spectra were recorded by coadding 20–100 scans. A sample from the source reactor or cold trap was then expanded into or flowed through the absorption cell. Spectra of

* Corresponding author. Fax: +1-303-497-5822.
E-mail address: burk@al.noaa.gov (J.B. Burkholder)
[1] Also associated with Cooperative Institute for Research in Environmental Sciences, University of Colorado, Boulder, CO 80309, USA.

1010-6030/00/$ – see front matter
PII: S1010-6030(00)00261-6

the sample, I, were recorded and absorption spectra calculated via $A=-\ln(I/I_0)$. The total pressure in the absorption cell for static measurements was in the range 1–10 Torr.

The NOAA apparatus also employed a residual gas analyzer quadrapole mass spectrometer (RGA-MS) for intensification of the cell contents and correlation with the UV absorption signals. The RGA-MS sampled the gas from the absorption cell through a 20 μm pinhole into a background pressure of $\sim 5\times10^{-5}$ Torr. The RGA-MS used electron impact ionization (70 eV) and covered the mass range 1–200 amu (0.5 amu resolution).

2.1. Materials

BrCl was prepared as described in previous studies [12] and stored in a glass reservoir at 195 K. Reagent grade HgO and Cl_2 was used as supplied. Br_2 was degased via freeze-thaw cycles and stored in a glass trap. N_2 (99.999%, UHP) was used as the flush gas. Pressures were measured using 10 and 100 Torr capacitance manometers.

3. Results and discussion

Fig. 1 shows a sequence of UV absorption spectra recorded at 100 s intervals of a static gas sample taken from the HgO source reactor. The spectra show the sample to contain a mixture of absorbing species with different time dependencies. Species Cl_2, BrCl, Br_2, OClO, Cl_2O, and Br_2O are expected to be present in the gas mixture and reference spectra, for these are shown in Fig. 2. At longer times, ~1 h, the spectra showed absorption due to just Cl_2, BrCl, and Br_2. Deconvolution of the absorption spectra as described below shows systematic increases in Cl_2, OClO, and BrCl and decreases in Br_2O, Cl_2O, and BrOCl (to be identified below). Br_2 was observed to increase although its changes were not well determined by the NOAA measurements due to its weak absorption in this measurement region.

The absorption peak centered at 272 nm in Fig. 1 is the only absorption feature which cannot be assigned to Cl_2, BrCl, Br_2, OClO, Cl_2O, or Br_2O (Fig. 2). During the course of the absorption measurements (~1 h), shown in Fig. 1, this feature decreased from an absorption of 1.4 to 0. The changes observed in the cell contents are initiated by D_2 lamp photolysis and the subsequent chemistry of the species in the cell. Test measurements showed the rate of change in the absorption spectrum to be dependent on the lamp exposure time and its intensity. We have used the time dependence in the absorbing species to identify the shape of the unidentified absorption feature and subsequently determine its absorption cross sections based on chlorine mass balance and the identification of the absorber as BrOCl.

3.1. Spectral analysis and identification of the BrOCl absorption spectrum

Fig. 2 shows reference spectra for Cl_2, BrCl, Br_2, OClO, Cl_2O, and Br_2O used in the spectral analysis. OClO is the

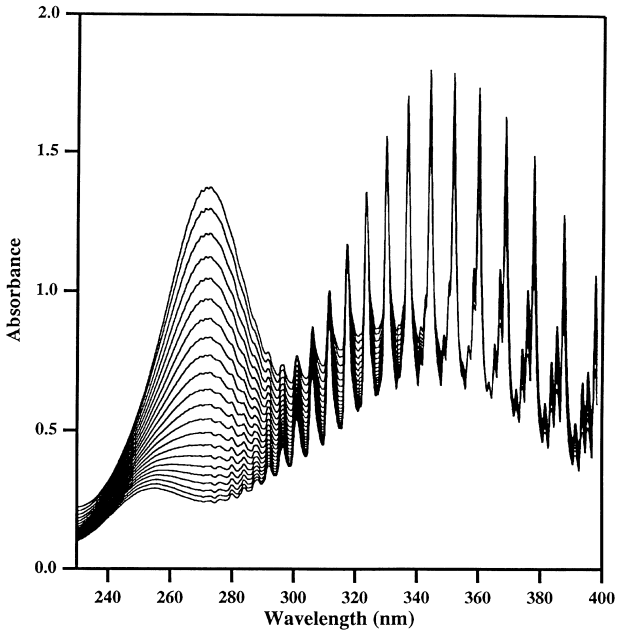

Fig. 1. Temporal evolution of the UV absorption spectrum at room temperature of a sample taken from the HgO reactor. Spectra were recorded at 100 s intervals with the earlier spectra showing maximum absorption at 272 nm. The spectra of how the loss of BrOCl (peak absorption at 272 nm) was accompanied by the formation of Cl_2, OClO, and BrCl (see text for details of spectrum analysis).

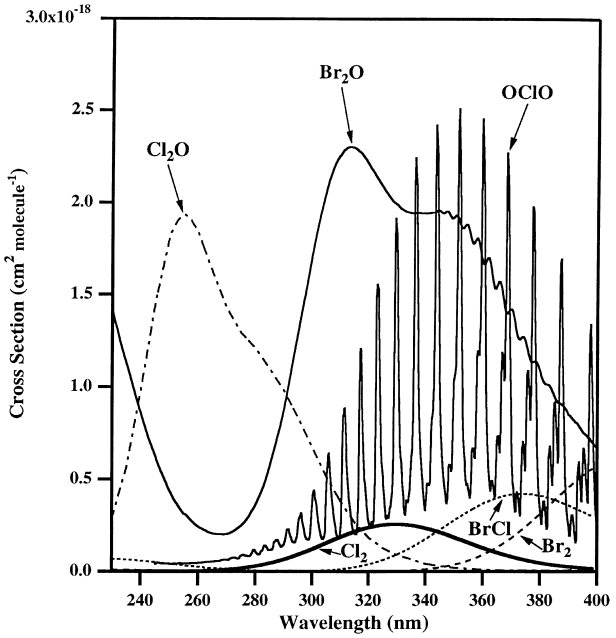

Fig. 2. Reference UV absorption spectra for Cl_2 (heavy solid line), BrCl (short dashed line), Br_2 (long dashed line), OClO (scaled by/5; structured spectrum), Cl_2O (dash-dot line), and Br_2O (solid line) used in the spectral analysis.

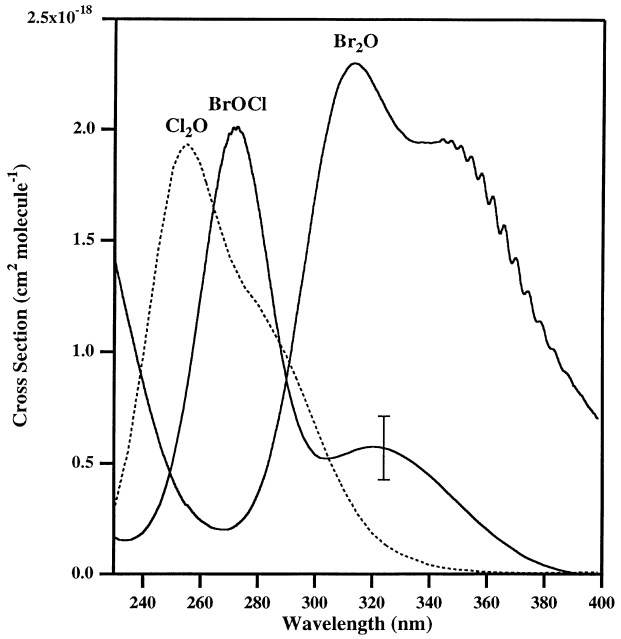

Fig. 3. Absorption spectrum of BrOCl (solid line) obtained from analysis of absorption spectra similar to shown in Fig. 1. Absorption spectra of Cl_2O and Br_2O (dashed lines) are also shown for comparison. The error bar represents our estimated uncertainty in the BrOCl cross section (∼25%) at all wavelengths based on the uncertainties in the mass balance analysis (see text).

most readily identifiable species in this system due to its pronounced vibrational band structure. The other species have relatively broad diffuse spectral shapes. However, accurate absorption measurements in this closed system (i.e. conservation of mass) with changing absorption signals for the various species provides sufficient information to determine the absorption spectrum of the unidentified species. Reference spectra were used to quantitatively subtract OClO, Cl_2, BrCl, Br_2, Cl_2O, and Br_2O from each spectrum (as described below) to yield a self-consistent shape for the residual absorption spectrum, BrOCl. The residual spectrum shows two peaks centered at 272 and 320 nm, Fig. 3. This spectrum was assigned to BrOCl via its correlation with the mass spectrometric measurements. The quantitative measurements of the chlorine containing species was used to determine the BrOCl absorption cross sections via mass balance.

The methodology and uncertainties in the determination of the BrOCl absorption spectrum following spectral subtraction of OClO, Cl_2, BrCl, Br_2, Cl_2O, and Br_2O are described below. A strong OClO absorption was present in the initial spectra and was present in all spectra which also contained BrOCl. The presence of OClO was not unexpected as it is also commonly observed as an impurity in the synthesis of Cl_2O by the HgO method. The OClO concentration was, however, relatively small and its prominence is due to its rather large absorption cross sections. The OClO and Br_2 spectral subtractions had only small effects, 1%, on the shape of the BrOCl spectrum except at wavelengths >370 nm. Br_2O was identified by its strong absorption at short wavelengths. Its contribution to the total absorption in the region of the BrOCl spectrum is small and decreased to zero after about 10 min. This decay greatly aided the identification of the Br_2O component. A significant fraction of the spectra in the analysis, therefore, contained no Br_2O. Therefore, Br_2O did not contribute to the uncertainties in the determination of the residual spectrum shape.

Cl_2O was identified using its absorption maximum at 250 nm. The Cl_2O subtraction has the largest influence on the spectral analysis over the wavelength range 240–280 nm. Initially Cl_2O accounts for ∼20% of the total absorption at 250 nm (see Fig. 1) and increases to ∼95% near the end of the measurement sequence. We estimate the accuracy of the Cl_2O subtractions to be ±10% leading to a ±5% uncertainty in the BrOCl absorption at 272 nm. Cl_2 and BrCl subtraction has the largest effect on the residual absorption shape at wavelengths >290 nm. BrCl was subtracted to obtain zero absorption at 400 nm.

In the time sequence spectra alone, the uncertainty in the Cl_2 subtraction is high due to the correlation between the Cl_2 spectrum and the BrOCl absorption peak at 325 nm. Therefore, a separate set of absorption measurements were made by trapping the output of the HgO source reactor at 200 K and pumping off the excess Cl_2. The trap was gradually warmed to ∼220 K while being pumped out through the absorption cell. Analysis of these spectra (with no Cl_2) showed the ratio of the BrOCl absorption at 320–272 nm to

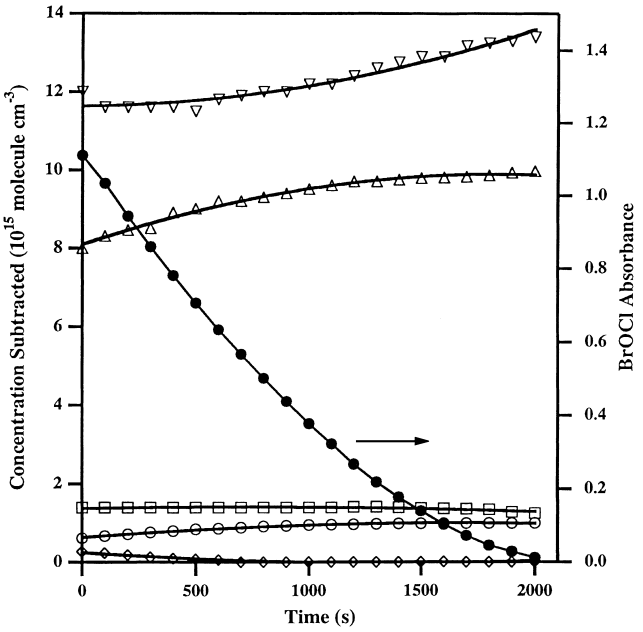

Fig. 4. Concentration profiles (temporal evolution) for Cl_2 (inverted triangle), BrCl (triangle), OClO (open circle), Cl_2O (square), and Br_2O (diamond) from the absorption spectra shown in Fig. 1. Also shown is the BrOCl absorption at 272 nm (solid circle) as a function of time. These data are used to determine the BrOCl absorption cross sections (shown in Fig. 3) via chlorine mass balance as described in the text.

Table 1
BrOCl absorption cross sections (10^{-18} cm^2 per molecule)

Wavelength (nm)	σ	Wavelength (nm)	σ
230	0.168	312	0.547
232	0.154	314	0.558
234	0.152	316	0.566
236	0.155	318	0.572
238	0.166	320	0.574
240	0.186	322	0.573
242	0.217	324	0.569
244	0.261	326	0.561
246	0.316	328	0.551
248	0.391	330	0.538
250	0.481	332	0.523
252	0.599	334	0.506
254	0.738	336	0.487
256	0.894	338	0.467
258	1.07	340	0.445
260	1.26	342	0.423
262	1.45	344	0.399
264	1.63	346	0.373
266	1.79	348	0.347
268	1.92	350	0.324
270	1.98	352	0.298
272	2.00	354	0.272
274	1.99	356	0.248
276	1.91	358	0.225
278	1.79	360	0.202
280	1.65	362	0.181
282	1.49	364	0.161
284	1.32	366	0.142
286	1.15	368	0.123
288	1.00	370	0.106
290	0.872	372	0.0866
292	0.763	374	0.0734
294	0.679	376	0.0612
296	0.616	378	0.0501
298	0.570	380	0.0400
300	0.540	382	0.0310
302	0.524	384	0.0230
304	0.521	386	0.0162
306	0.523	388	0.0103
308	0.530	390	0.0055
310	0.539		

be 0.287 (±10%). Cl_2 was subtracted from the time dependent spectra to obtain this same ratio. Fig. 3 shows the resulting averaged BrOCl absorption spectrum obtained from the analysis of the time sequence shown in Fig. 1. The relative shape of the BrOCl spectrum obtained from an individual spectrum agreed with the average to better than 5% over the entire wavelength range.

Using the spectral subtractions discussed above, Fig. 4 shows the time evolution of the concentrations for OClO, Cl_2, BrCl, Cl_2O, and Br_2O from the spectra shown in Fig. 1. The absorption cross sections for these species were taken from the literature which is summarized in DeMore et al. [14] for OClO, Cl_2, BrCl, and Cl_2O. Data for Br_2O was taken from Orlando and Burkholder [5]. Also shown in Fig. 4 is the decrease in the BrOCl absorption at 272 nm with time. Fig. 4 shows significant increases in both Cl_2 and BrCl, small changes in OClO and Cl_2O, and a complete loss of Br_2O. Using chlorine mass balance we determined the absorption cross sections of BrOCl shown in Fig. 3 and listed in Table 1. Other measurement sets with different initial concentrations showed similar concentration profiles and yielded consistent BrOCl cross sections. Our limited accuracy of the Br_2 measurement, ±50%, precluded using bromine mass balance in the cross section determination.

We estimate the overall accuracy of the BrOCl absorption cross section to be ±25% while the relative cross sections (wavelength dependence) are expected to be more accurate, ±10%. Also shown in Fig. 3 for comparison are the absorption spectra for Cl_2O and Br_2O. It is reasonable to expect the peak absorption cross section for BrOCl to fall between those of Cl_2O and Br_2O as shown in Fig. 3. This is consistent with the absorption cross sections for BrCl when compared to Cl_2 and Br_2 (see Fig. 2). We believe the spectral analysis presented above to be self-consistent and allows the BrOCl absorption spectrum to be normalized if and when more accurate values become available.

3.2. Gas phase identification of BrOCl

A series of measurements were performed in which the gas sample from the HgO reactor was collected in a trap at liquid nitrogen temperature before entering the absorption cell. The temperature of the trap was gradually raised and the eluting material was pumped through the absorption cell.

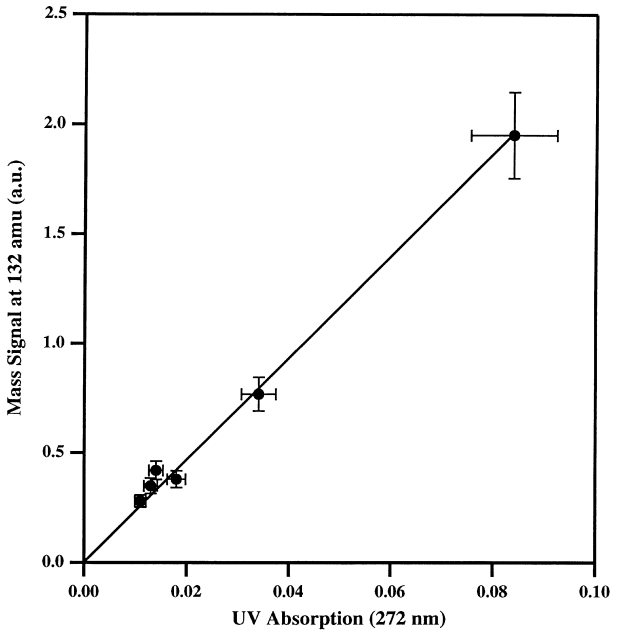

Fig. 5. Correlation of the mass spectrum signal at 132 amu (BrOCl) to the UV absorption signal at 272 nm (BrOCl) following the spectral subtractions as described in the text. The solid line is a least squares fit to the data. The error bars represent the estimated uncertainties, ±10%, in the mass spectrum and UV absorption signals.

The total pressure in the absorption cell was <0.15 Torr. Absorption and mass spectra of the gas were made simultaneously during this time. We observed the species by UV absorption and mass spectra to elute from the trap in the order: Cl_2, OClO, Cl_2O, BrCl, BrOCl, Br_2, and Br_2O. However, the species were at no time completely isolated in the absorption cell until relatively pure Br_2O was present as the sample was nearly depleted. BrOCl was identified in the mass scans by its isotopic fingerprint and intensity ratio of 3:4:1. The measured intensity ratio values were 3.38±0.14:4:0.99±0.09 for the masses 130:132:134 where the error limits are 1σ of the measurement precision. Also the intensity of the mass scans was well correlated (±10%), Fig. 5, with the BrOCl absorption at 272 nm over the concentration range $(0.5–4.5)\times10^{14}$ molecule cm^{-3}.

Acknowledgements

This work is supported in part by the NASA upper atmosphere research program. NCAR is operated by the University Corporation for Atmospheric Research under the sponsorship of the National Science Foundation.

References

[1] C.L. Lin, J. Chem. Eng. Data 21 (1976) 411.
[2] J.B. Nee, J. Quant. Spectrosc. Radiat. Transfer 46 (1991) 55.
[3] C.M. Nelson, T.A. Moore, M. Okumura, J. Chem. Phys. 100 (1994) 8055.
[4] S.L. Nickolaisen, C.E. Miller, S.P. Sander, M.R. Hand, I.H. Williams, J.S. Francisco, J. Chem. Phys. 104 (1996) 2857.
[5] J.J. Orlando, J.B. Burkholder, J. Phys. Chem. 99 (1995) 1143.
[6] O.V. Rattigan, D.J. Lary, R.L. Jones, R.A. Cox, J. Geophys. Res. 101 (1996) 23021.
[7] D.M. Rowley, M.H. Harwood, R.A. Freshwater, R.L. Jones, J. Phys. Chem. 100 (1996) 3020.
[8] J.B. Burkholder, Int. J. Chem. Kinet. 30 (1998) 571.
[9] T. Lee, J. Phys. Chem. 99 (1995) 15074.
[10] M. Bahou, L. Schriver-Mazzuli, A. Schriver, P. Chaquin, Chem. Phys. 216 (1997) 105.
[11] J.B. Burkholder, J. Geophys. Res. 98 (1993) 2963.
[12] J.B. Burkholder, A.R. Ravishankara, S. Solomon, J. Geophys. Res. 100 (1995) 16793.
[13] T.A. Staffelbach, J.J. Orlando, G.S. Tyndall, J.G. Calvert, J. Geophys. Res. 100 (1995) 14189.
[14] W.B. DeMore, S.P. Sander, D.M. Golden, R.F. Hampson, M.J. Kurylo, C.J. Howard, A.R. Ravishankara, C.E. Kolb, M.J. Molina, Chemical Kinetics and Photochemical Data for Use in Stratospheric Modeling. Evaluation No. 11, JPL Publication 97-4, Jet Propulsion Laboratory, Pasadena, CA, 1997.